E

I
m
s
I
t
e
a
a
m
t

-
-

that allows growth and stabilization of the developing thrombus. Initiation of the coagulation cascade essentially relies on the presence of a procoagulant phospholipid surface and the glycoprotein tissue factor (TF; Nemerson, 1968). These two components initiate the sequential assembly and activation of the membrane-associated prothrombinase complex (factor Xa [FXa] and factor Va; Nemerson, 1968), which generates thrombin, the serine protease that converts brinogen to brin, and thereby provides the backbone of the growing thrombus (Wolberg, 2007).

Although all cellular membranes contain abundant amounts of phospholipids, they are usually inert and do not support coagulation. Platelets are considered to serve as a major source of procoagulant phospholipids, as these cells can actively modify their membrane and oxidize and externalize the aminophospholipids phosphatidylethanolamine (PE) and phosphatidylserine (PS; Suzuki et al., 2010; Thomas et al., 2010; Yang et al., 2012; O'Donnell et al., 2014). Although platelets can potentially acquire TF via leukocyte-derived microparticles, they lack endogenous expression of TF (Bouchard et al., 2010). These ndings raise the question about the exact mechanisms and cells that initiate the assembly of the prothrombinase complex during the onset of coagulation and the propagation of intravascular thrombosis (Flaumenhaft, 2014).

Here, we report that thrombotic events in humans are associated with an in increase in the eosinophilic activation marker eosinophilic cationic protein (ECP). Subsequent experiments showed that eosinophils were abundantly found in thrombi that formed upon vascular injury in mice, where these (as a ee)20(v6(haft,)120(e00.5(3b)15.1(uted to thr)

the thrombus (Fig. 2, A and B; and Fig. S1, A–E). To determine whether eosinophils actively 120(e)-44.9(ib)15(uted to the foe)-45(m
an injury-induced venous thrombosis model of the infeeior venae cava (IVC) in two di erent eosinophil-de cient mouse strains, namely Δ

dblGATA1 mice (Yu et al., 2002) and PHIL mice (Lee et al., 2004), as well as in their WT litteemates.

thrombus foemation (Fig. 2, C and D), wh3ch supported a functionaf 120(e)-45(ib)15(ution of these cells.)100.1( )80.3(Also)50(,)10
body showed a signi cantt,eased thrombotic potentiaf (Fig. 2 E and Fig. S1 F).

As these dataward a so far unrecognized role of eosinophils dueing the initiation and/or propagation of thrombosis, we sought to elucidate the underlying mechanisms. We did not observe alterations in platelet numbers or platelet function or any intrinsic defects of clotting factors in eosinophil-de cient mice (Fig. S2, A–C). However, measurement of plasmatic thrombin–antithrombin (TAT) complexes as a quantitative marker foe thrombin generation showed that TAT complexes rapidly appeared after induction of thrombosis in WT mice but were almost absent in eosinophil-de cient mice (Fig. 2 F). These dataereve of a majoe 120(e)-45(i)]TJ0 Tw (-)Tj0.07
aggregation and thrombus foemation upon vascular injury in the mouse carotid arteey of WT and eosinophil-de cient

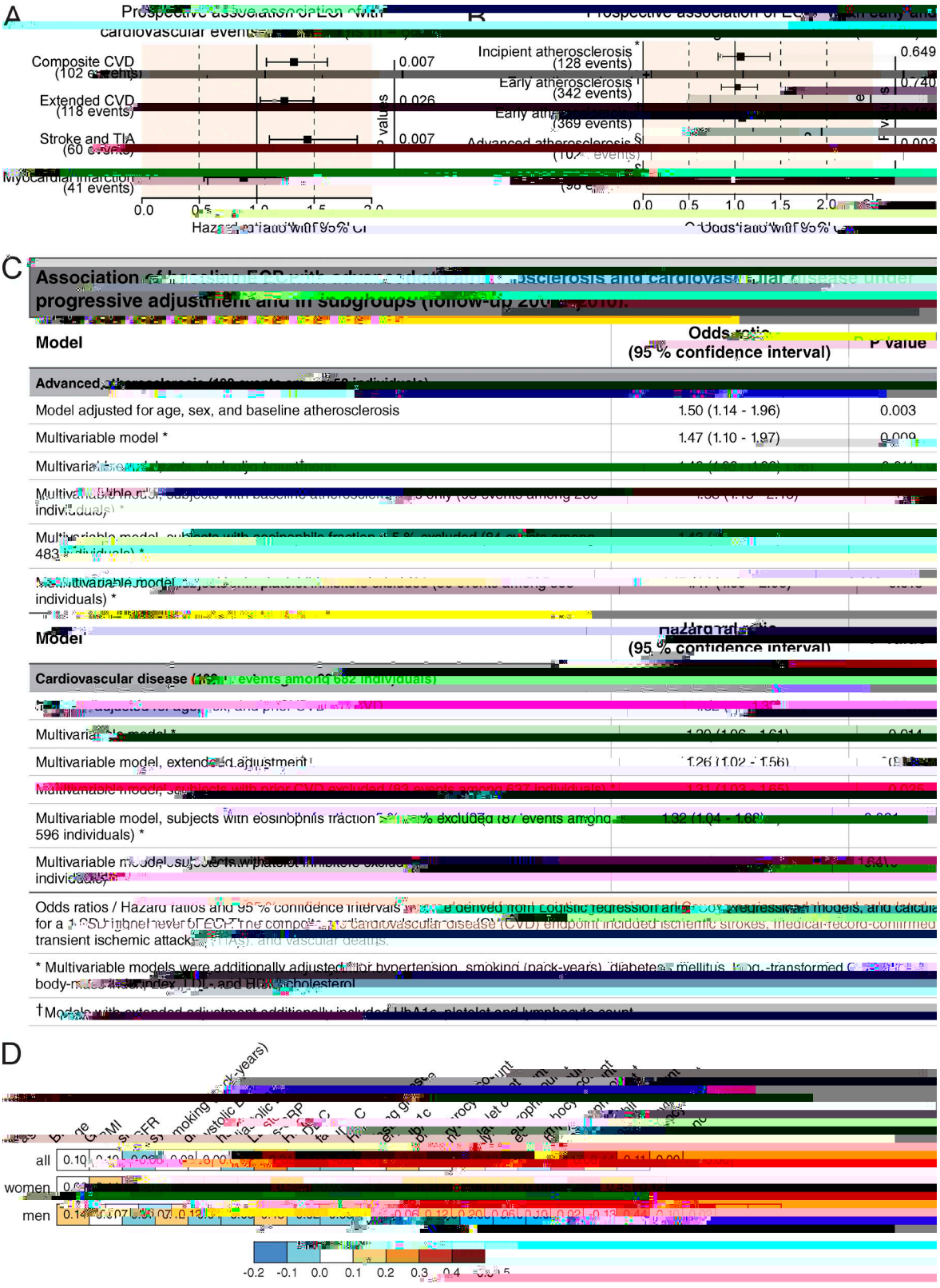

Figure 1. **Elevation of ECP serves as a marker for CVD in humans.** (A and B) Forest plots of the prospective association of baseline ECP with events of CVD (A) and early and advanced atherosclerosis (B) in the Bruneck Study (follow-up 2000 to 2010). All analyses were adjusted for age, sex, and prior CVD. Analyses focusing on ultrasound endpoints were adjusted to the extent of baseline atherosclerosis (log-transformed atherosclerosis summation score).

mice. Whereas an absence of eosinophils did not impair the

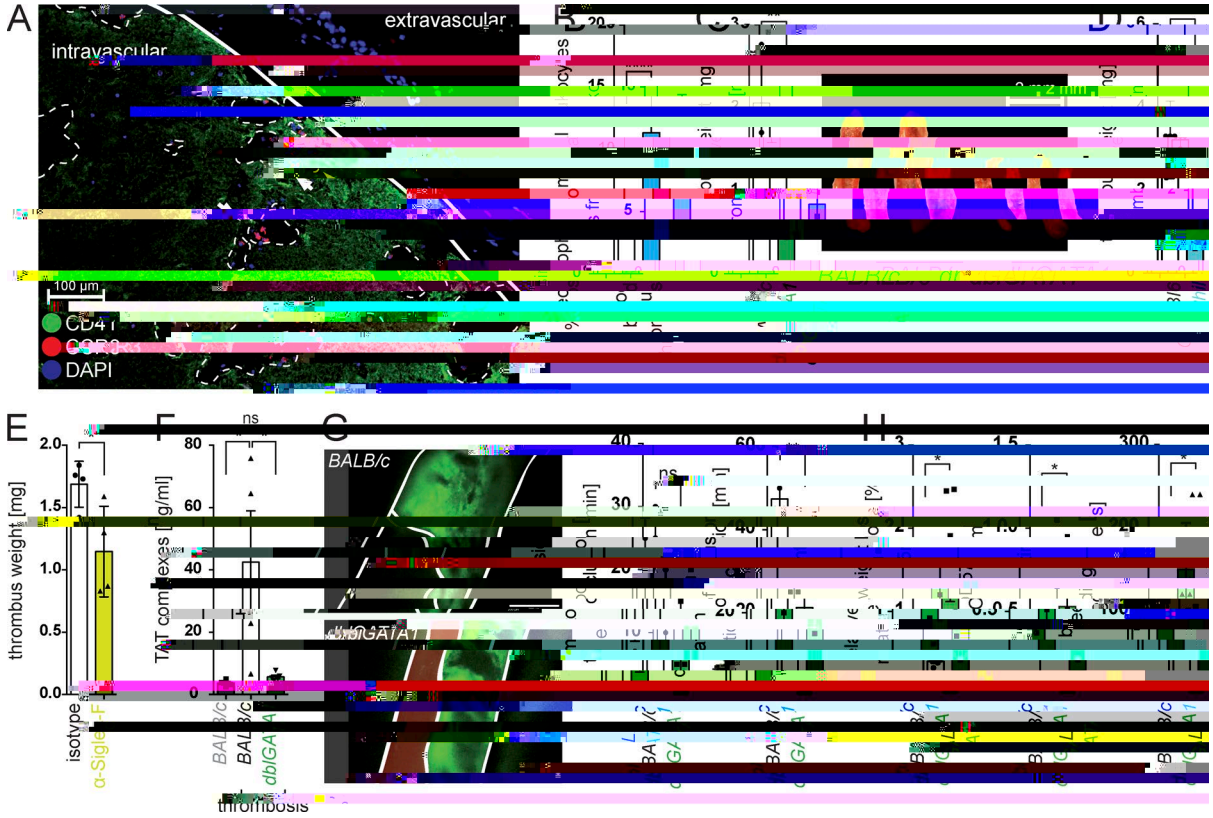

Figure 2. **Eosinophils contribute to intravascular thrombosis and hemostasis.** (A) Representative microscopy image (n = 5) showing immuno□u-orescence staining for platelets (CD41; green), eosinophils (CCR3; red), and cellular nuclei (DAPI; blue) in a ferric chloride (FeCl)–induced thrombus of a mouse IVC. White arrowheads indicate CCR3$^+$ eosinophils, and dashed lines mark lacunae surrounded by platelet aggregates. Bar, 100 µm. (B) Relative number of eosinophils in IVC thrombi of WT mice compared with peripheral blood counts. n = 5. (C and D) FeCl-induced IVC thrombus of Δ*dblGATA1* mice (BALB/c background; n = 4; C), PHIL mice (C57BL/6 background; n = 10; D), and their corresponding WT littermates. Bar, 2 mm. (E) FeCl-induced IVC thrombosis in WT mice treated with anti-SiglecF antibody (n = 4) or isotope control. (F) Measurement of TAT complexes in plasma from *dblGATA1* mice (n = 5) after FeCl-induced IVC thrombosis. (G) Representative image of a FeCl-induced thrombosis of the carotid artery in WT or Δ*dblGATA1* mice (30 min after FeCl-induced injury) and quanti□cation of the kinetics of thrombus formation and dissolution (right; see also supplementary videos). n = 4. Bars, 200 µm. (H) Bleeding assays (15-mm tail cut) with WT (*BALB/c*; n = 5) and Δ*dblGATA1* mice (n = 9). Bar graphs show relative weight loss, OD_{575nm} of the lost blood after lysis, and primary bleeding time (time until the □rst stop of bleeding). Data are representative of at least three independent experiments. Error bars represent SEM. *, P < 0.05; **, P < 0.01; ***, P < 0.001; ****, P < 0.0001; Student's t test.

membrane (Suzuki et al., 2010; Tian et al., 2012; Yang et al., 2012; Kunzelmann et al., 2014). Also, eosinophils expressed several TMEM family members (Fig. S3 D), and the Ca^{2+} ionophore A23187 rapidly triggered exposure of the aminophospholipids PE and PS in eosinophils (Fig. 4 D and Fig. S3 E). Intracellular chelation of Ca^{2+} by BAPTA/AM or addition of tannic acid, a nonselective inhibitor of the TMEM family of calcium-activated Cl^- channels, in turn, interfered with the ADP-induced binding of annexin V to their surface (Fig. 4 E). In line with these □ndings, ADP stimulation of eosinophils triggered a rapid and transient increase in cytosolic Ca^{2+} levels in a Ca^{2+}-free environment, which could be boosted by the addition of extracellular calcium (Fig. 4 F). Prior depletion of intracellular calcium stores by thapsigargin, an inhibitor of the endoplasmic reticulum Ca^{2+} ATPase, blocked the initial ADP-induced increase in cytosolic Ca^{2+} (Fig. 4 G). These data were suggestive of an initial ADP-induced Ca^{2+} release from intracellular stores and a subsequent activation of a store-operated calcium entry through the plasma membrane (Bergmeier et al., 2013) that triggered exposure of procoagulant aminophospholipids to immediately support TF-dependent formation of the prothrombin complex (Fig. 4 H).

12/15-LO–mediated formation of procoagulant oxidized phospholipids essentially contributes to the thrombin-generation potential of eosinophils

Next, we aimed to determine whether speci□c aminophospholipid species accounted for the increased thrombin-generation potential of eosinophils and performed an additional lipidomic analysis of their phospholipid pro□le, which showed that their cellular membranes were enriched in a speci□c set of

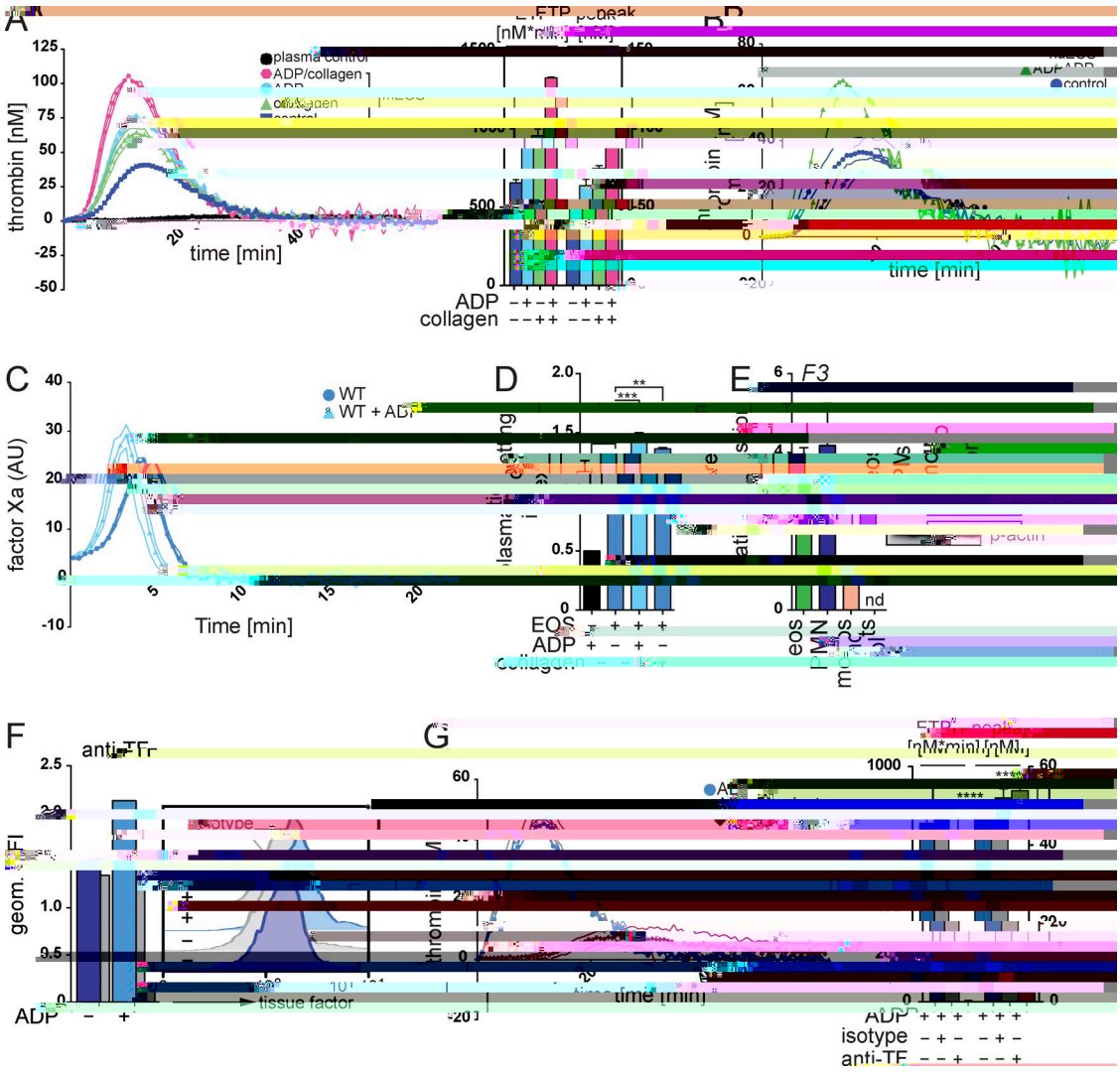

Figure 3. **Eosinophils autonomously initiate thrombin generation.** (A and B) Calibrated thrombin generation curve of in vitro–generated mouse eosinophils (mEOS; A) or human eosinophils (huEOS; B) after stimulation with ADP and/or collagen. Bar graphs show endogenous thrombin potential (ETP; nM*min) and peak of thrombin generation (peak; nM). (C) Calibrated FXa generation curve of mouse eosinophils. AU, arbitrary units. (D) Plasma clotting time experiments with in vitro–generated mouse eosinophils (Eos) stimulated with ADP or collagen. Bar graphs display calculated clotting index. The black bar shows plasma with ADP alone. (E, left) Quantitative RT-PCR analysis of TF mRNA (*F3*) expression in mouse monocytes (monos), neutrophils (PMN), eosinophils (eos), and platelets (plts); expression of the gene of interest was normalized to *Atcb* expression. (Right) Western blot analysis of TF protein (47 kD) expression in sorted mouse leukocytes. (F) Flow cytometry analysis of the exposure of TF on the surface of resting or ADP-stimulated mouse eosinophils. Histograms show representative flow cytometric stainings, and bar graphs show mean geometric fluorescence intensities (geom. MFI). (G, left) Calibrated thrombin generation assay with ADP-stimulated mouse eosinophils in the presence of blocking anti-TF antibody or isotope control. (Right) Bar graphs show endogenous thrombin potential (ETP; nM*min) and peak of thrombin generation (peak; nM). Data are representative of at least three independent experiments. Error bars represent SEM. *, $P < 0.05$; **, $P < 0.01$; ***, $P < 0.001$; ****, $P < 0.0001$; Student's *t* test.

PE oxidation products (12–hydroxyeicosatetraenoic acid–PEs [12-HETE-PEs]; Fig. 5 A). As oxidation of phospholipids had been suggested to increase their procoagulant potential (Thomas et al., 2010), we sought to determine a potential role of PE oxidation and the different oxidized PE species during eosinophil-mediated thrombin generation. 12-LO (*Alox12*) and 12/15-LO (*Alox15*) are the two major enzymes exerting 12-LO activity in mammals (Kuhn et al., 2015) and thus served as the potential enzymatic source for the identified 12-HETE-PEs in eosinophils. Analysis of peripheral blood leukocytes and platelets showed that *Alox12* was absent in all leukocyte subsets and exclusively expressed in platelets. *Alox15* mRNA and 12/15-LO protein, in turn, were highly expressed in mouse and human eosinophils but absent in platelets, monocytes, neutrophils, and the healthy vascular wall (Fig. 5, B–D; and Fig. S3 F). These data showed that, during the steady state,

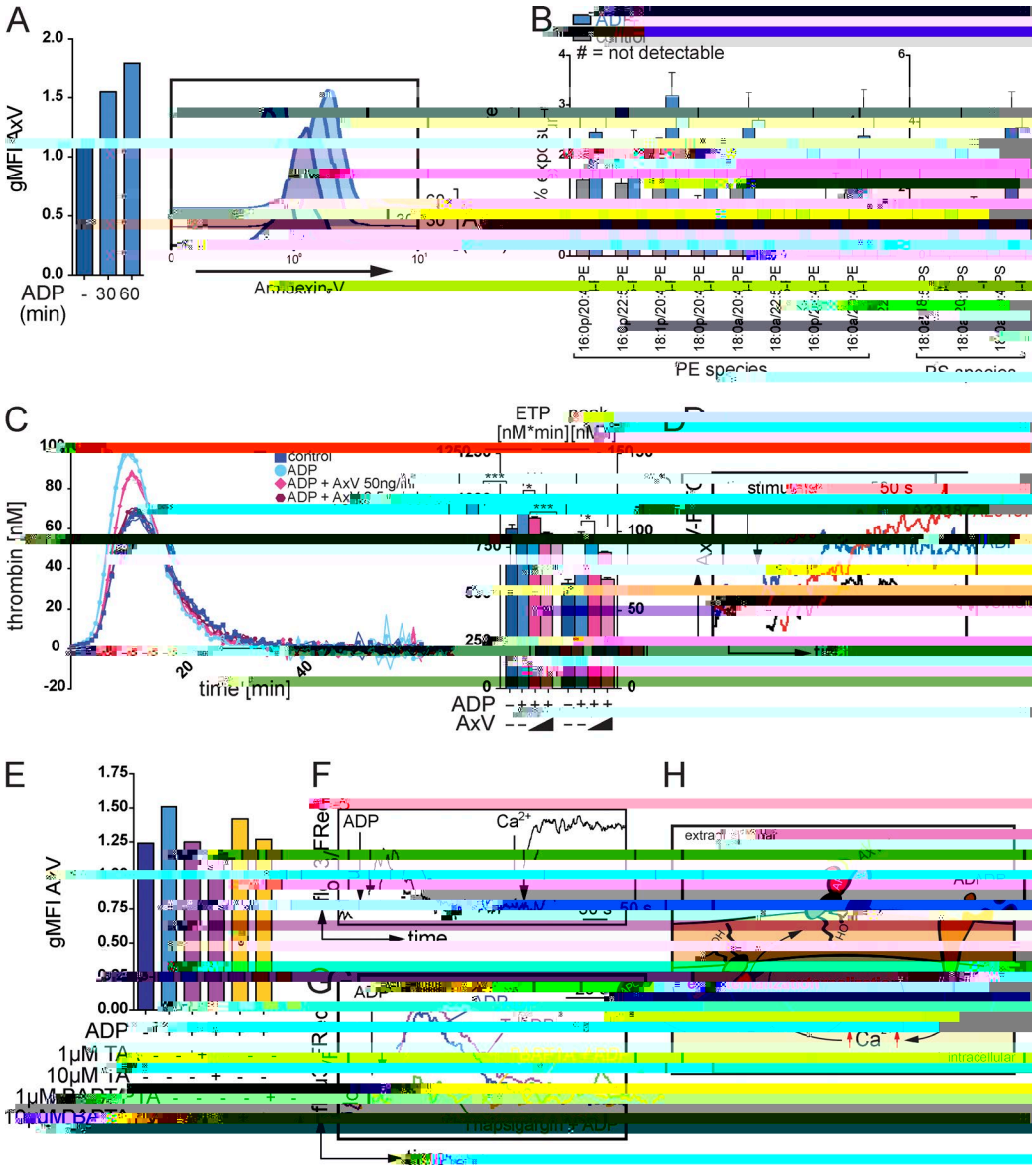

Figure 4. Ca^{2+}-dependent exposure of aminophospholipids by eosinophils promote thrombin generation. (A) Flow cytometry analysis of the binding of annexin V (AxV) to aminophospholipids on the surface of resting or ADP-stimulated mouse eosinophils. Histograms show representative annexin

eosinophils were the only cells expressing *Alox15* within the peripheral blood and the vasculature. 12/15-LO expression was accordingly absent in blood leukocytes of 12/15-LO–de cient (*Alox15*$^{-/-}$) and eosinophil-de cient Δ*dblGATA1* mice (Fig. 5, E and F). Mass spectrometry showed that *Alox15*$^{-/-}$ eosinophils indeed lacked the identi ed 12-HETE-PEs, thus con rming 12/15-LO as the single enzymatic source of these oxidized aminophospholipids in eosinophils (Fig. 5 G).

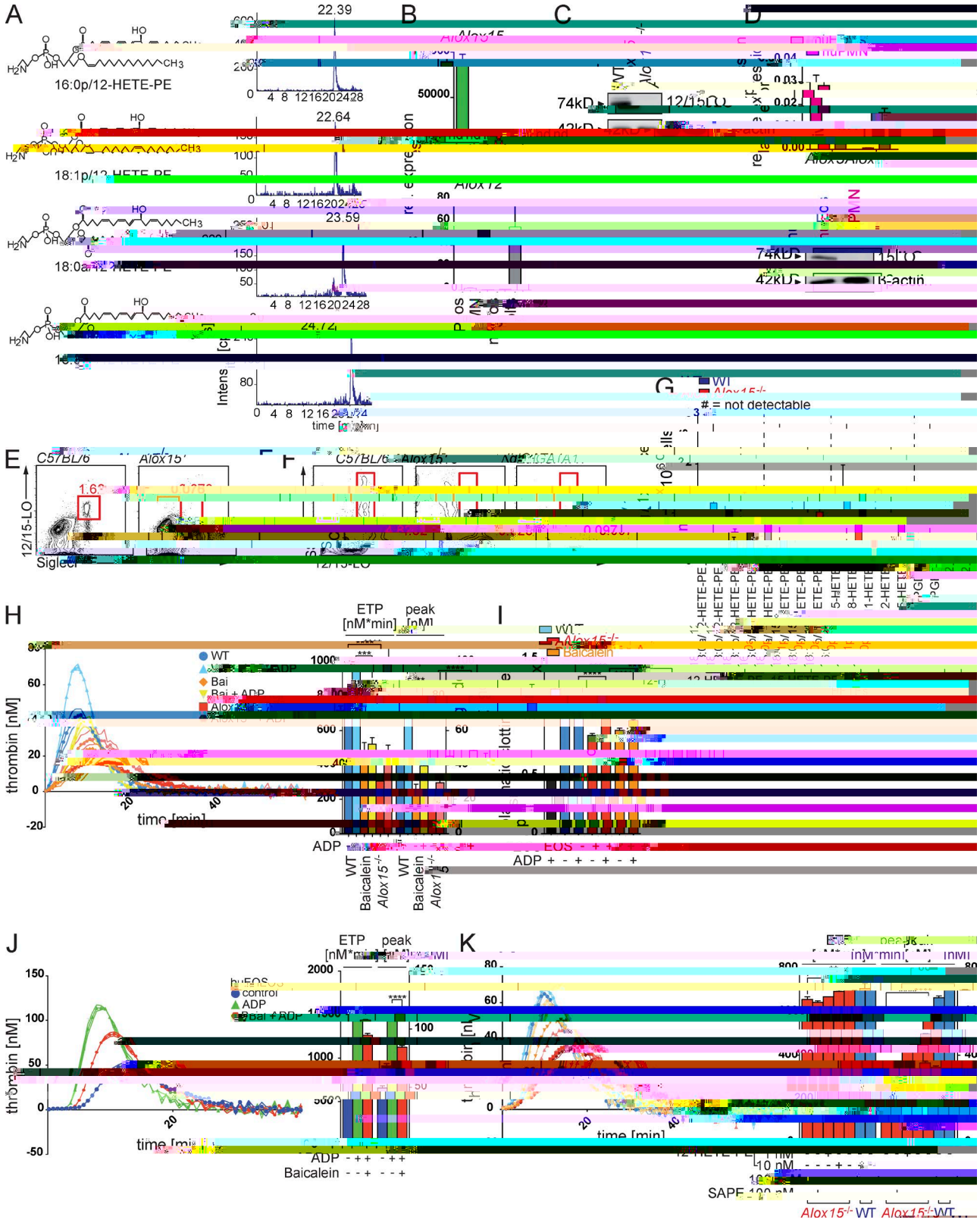

Figure 5. **12/15-LO–mediated oxidation of membrane phospholipids initiates eosinophil-mediated thrombin formation.** (A) Representative LC/MS/MS analysis of different 12-HETE-PE oxidation species in lipid extracts of in vitro–generated mouse eosinophils. Cps, counts per second. (B) Quantitative RT-PCR analysis of 12/15-LO mRNA (*Alox15*) and 12-LO mRNA (*Alox12*) in mouse monocytes (monos; CD11b$^+$CD115$^+$), neutrophils (PMN; CD11b$^+$Ly6G$^+$),

In accordance with a major contribution of 12/15-LO–mediated membrane oxidation to the thrombin-formation activity of eosinophils, we observed a severely reduced ability of *Alox15*$^{-/-}$ eosinophils to generate thrombin and FXa as well as to induce brin clots (Fig. 5, H and I; and Fig. S3 G). The 12/15-LO inhibitor baicalein potently interfered with the procoagulant activity of mouse and human eosinophils as well (Fig. 5, H–J), showing that the *Alox15*-mediated control of plasma coagulation by eosinophils represented an evolutionary conserved mechanism and potential target for pharmacologic intervention during thrombotic disease. Of note, 12/15-LO–de cient eosinophils showed no alterations in their eosinophil maturation markers (Fig. S3, H and I). Phospholipase A2 (PLA2)–dependent cleavage of 12/15-LO products from membrane phospholipids was not involved in the 12/15-LO–mediated thrombin generation activity of eosinophils, as inhibition of PLA2 activity did not reduce the procoagulant activity of eosinophils (Fig. S3 J).

We subsequently measured thrombin generation in the presence of liposomes containing di erent PE species to substitute for 12/15-LO activity. Addition of liposomes with 12-HETE-PE immediately restored the thrombin-generation potential of *Alox15*$^{-/-}$ eosinophils, whereas identical liposomes with nonoxidized PEs were ine ective (Fig. 5 K), supporting the concept of a 12/15-LO–mediated control of thrombin generation that was dependent on generation and provision of 12-HETE-PEs.

12/15-LO expression in eosinophils promotes thrombotic disease and supports physiological hemostasis

neutrophils and monocytes in the peripheral blood seem to be unable to provide an enzymatically engineered, procoagulant phospholipid surface, whereas platelets express prothrombotic phospholipids but lack intrinsic TF expression. Thus, eosinophils seem to combine the abilities of platelets to oxidize and expose distinct prothrombotic aminophospholipids with

genesis of atherosclerosis that started in 1990. The study population was recruited as a sex- and age-strati ed random sample of all residents age 40 to 79 living in Bruneck (n = 4,739), Northern Italy. Detailed follow up examinations including high-resolution ultrasound of the carotid vessels were performed every 5 yr. The present analysis focuses on the evaluation in 2000 (n = 682 with complete data including carotid ultrasound), which served as the baseline for this analysis, and on the 10-yr follow-up period between 2000 and 2010. Follow-up for clinical endpoints was 100% complete (n = 682, mean and median follow up time 8.6 and 10 yr), whereas follow up ultrasound examinations in 2005 and 2010 were available in 558 men and women (i.e., 91.9% of survivors or 81.8% overall). The study protocol was approved by the Ethics Committees of Verona and Bolzano, and all participants gave their written informed consent before entering the study.

All risk factors were assessed by means of validated standard procedures described previously (Kiechl et al., 2002, 2013; Stegemann et al., 2014). In brief, body mass index was calculated as weight divided by height squared (kg/m^2). Hypertension was de ned as blood pressure ≥140/90 mm Hg (mean of three independent readings obtained with a standard mercury sphygmomanometer after at least 10 min of rest) or the use of antihypertensive drugs. Lifetime smoking was assessed as pack-years. Diabetes was de ned based on American Diabetes Association criteria.

The composite CVD endpoint was composed of ischemic stroke, medical record–con rmed transient ischemic attack (TIA), myocardial infarction, and vascular death. A total of 102 individuals experienced primary outcome events. The extended composite endpoint additionally considered revascularization procedures, which increased the number of individuals a ected to 118. Myocardial infarction was deemed con rmed when World Health Organization criteria for de nite disease status were met. Ischemic stroke and TIA were classi ed according to the criteria of the National Survey of Stroke. A TIA was considered only if the diagnosis could be made with high accuracy (medical record–con rmed TIA). All revascularization procedures (angioplasty and surgery) were carefully recorded. Ascertainment of events or procedures did not rely on hospital discharge codes or the patient's self-report but on a careful review of medical records provided by the general practitioners, death certi cates, Bruneck Hospital les, and the extensive clinical and laboratory examinations performed as part of the study protocols. Major advantages of the Bruneck Study are that virtually all subjects living in the Bruneck area were referred to the local hospital and that the network existing between the local hospital and the general practitioners allowed retrieval of practically all medical information on persons living in the area. We also collected detailed information on the date, causes, and circumstances of death for all study subjects who did not survive the entire follow-up period by consulting death certi cates, all medical records ever compiled on study subjects, and autopsy reports in the rare event of unexpected death. We were able to ascertain 100% of deaths and reliably classify them as vascular deaths, cancer deaths, or deaths from other causes (primary cause of death). Vascular mortality included deaths from ischemic stroke, myocardial infarction, rupture of aortic aneurysms, and sudden cardiac deaths. The experienced researcher who categorized all deaths and cardiovascular endpoints was unaware of laboratory data. There was no loss of follow-up for clinical endpoints.

Assessment of atherosclerosis. At each study visit, participants underwent bilateral carotid duplex sonography using a 10-MHz transducer and a 5-MHz Doppler. All subjects were examined in supine position. The scanning protocol involved four segments of the right and left carotid artery: proximal common carotid artery (15–30 mm proximal to the carotid bulb), distal common carotid artery (<15 mm proximal to the carotid bulb), proximal internal carotid artery (carotid bulb and the initial 10 mm of the vessel), and distal internal carotid artery (>10 mm above the ow divider). A plaque was de ned as a focal structure encroaching into the arterial lumen with a thickening of the vessel wall of at least 0.5 mm relative to surrounding segments. The maximum axial diameter of plaques (in millimeters) was assessed on the near and far walls at each of the eight vessel segments. The atherosclerosis summation score was calculated by summing all diameters (intraobserver coe cient of variation, 13.5%; n = 100).

A person-based atherosclerosis progression model (Kiechl and Willeit, 1999a; Kiechl et al., 1999b) was developed and validated in the Bruneck Study that allowed di erentiation between early and advanced stages in atherosclerosis development (Kiechl et al., 2013). Early atherosclerosis subsumes the manifestation of new plaques and/or nonstenotic progression of existing plaques. Main characteristics are a slow and continuous plaque growth, usually a ecting more than one plaque simultaneously and accompanied by a compensatory or even overcompensatory enlargement of the vessel at the plaque site. The term incipient atherosclerosis was used for the development of rst plaques in subjects free of atherosclerosis at baseline (Kiechl et al., 2002). Advanced complicated atherosclerosis was assumed when the relative increase in the maximum plaque diameter exceeded twice the measurement error for the method (internal carotid artery, 25%; common carotid artery, 17%) and a lumen narrowing of at least 40% was achieved. This process is featured by a usually solitary prominent increase in plaque size and absence of vascular remodeling, thus resulting in signi cant lumen compromise. From a mechanistic perspective, it refers to plaque destabilization and subsequent atherothrombosis (Willeit et al., 2000).

The two progression categories were highly reproducible (κ coe cients > 0.8 [n = 100]). Risk pro les di er signi cantly between the two stages of carotid artery disease with early atherosclerosis relying on standard risk factors and advanced atherosclerosis being mainly related to markers re ecting plaque vulnerability or enhanced prothrombotic activity (Willeit et al., 2000; Kiechl et al., 2007).

Statistical methodology. We tested the hypothesis that baseline ECP level is associated with new-onset CVD and advanced atherosclerosis (2000–2010), both of which rely on atherothrombosis, but not with early atherosclerosis driven by in ammation and standard vascular risk factors. Cox proportional hazard models with progressive adjustment were used to analyze time-to-event data on the primary CVD endpoint (ischemic strokes, medical record–con rmed TIAs, myocardial infarctions, and vascular deaths), extended CVD endpoint (plus revascularization procedures), and individual disease endpoints (stroke and TIA or myocardial infarction; Fig. 1 A). Subjects who su ered a CVD event were censored with respect to subsequent follow-up as were participant who died from nonvascular causes. We detected no departure from the proportional hazards assumption by inspecting Schoenfeld residuals and checking the parallelism of log–log survival plots. Associations between ECP and the various measures of atherosclerosis were tested by means of logistic regression analysis (Fig. 1 B) because the quinquennial examinations in the Bruneck Study provide reliable information on plaque development/progression in this time interval but no time-to-event information.

Base models were adjusted for age, sex, and either prior CVD (CVD endpoints) or baseline atherosclerosis (ultrasound endpoints). Multivariable analyses were additionally adjusted for hypertension, smoking (pack-years), diabetes, $\log_e$-transformed C-reactive protein, body-mass index, and LDL and high-density lipoprotein (HDL) cholesterol. We modeled ECP as a continuous variable and calculated hazard and odds ratios for a 1-SD unit–higher level of ECP.

In subsidiary analyses, we excluded subjects with prior CVD, eosinophil fractions >5%, or platelet inhibitor therapy. All p-values were two sided, and an α level of 0.05 was used. Analyses were conducted using SPSS and R 3.2.2 (R Foundation for Statistical Computing).

Proteomic serum analysis. Blood samples were drawn in the year 2000 after an overnight fast and 12 h of abstinence from smoking and immediately frozen and stored at −70°C (without any thawing-freezing cycle). Laboratory parameters were measured by standard assays, and a blood di erential was performed using an automated analyzer (Kiechl et al., 2002, 2013; Stegemann et al., 2014). Eosinophil cationic protein (ECP) was measured in plasma samples collected in the year 2000 as part of a novel proteomics chip (Proximity Extension Assay; 4 Proseek Multiplex CVD I96 × 96; Olink Bioscience) as described previously (Assarsson et al., 2014).

Animals

Animal experiments were approved by the government of Mittelfranken, the Mayo Clinic, and the Ludwig Maximilian University, Munich. 12/15-LO–de cient (*Alox15*$^{-/-}$; C57BL/6 background), ΔdblGata1 (BALB/c background), and PHIL mice were described previously (Yu et al., 2002; Lee et al., 2004). ΔdblGata1mice carry a deletion of a high-a nity GATA-binding site in the GATA-1 promoter (Δ*dblGATA-1* mice), whereas PHIL mice express a diphtheria toxin A transgene that is driven by a fragment of the eosinophil peroxidase promoter. Both mouse strains show a selective and complete absence of the eosinophilic lineage. To achieve an eosinophil-speci c deletion of *Alox15*, we crossed an EPX-Cre mouse (Doyle et al., 2013) with mice carrying oxed Alox15 alleles (both C57BL/6 background; Cole et al., 2012). Experiments were performed at an age of 8–10 wk. Whereas experiments with Δ*dblGATA-1* mice were performed in hemizygous mutant males and WT male littermates, the experiments with other mouse strains were performed with an equal gender distribution of mutant and WT mice. Animal experiments were performed by a blinded investigator.

Cell culture

Eosinophils were generated from bone marrow isolated from 8-wk-old mice as previously described (Dyer et al., 2008) with minor modi cations. In brief, bone marrow was incubated in RPMI medium (Gibco) containing 20% heat-inactivated feral calf serum (FCS), 25 mM Hepes, 100 IU/ml penicillin (Gibco), 10 µg/ml streptomycin (Gibco), 2 mM glutamine (Gibco), 1× nonessential amino acids (NEAA;

added and incubated for 10 min at 37°C. End concentration of ADP (Roche) was 40 µM. Then, 20 µl of recalci cation solution containing a uorogenic substrate for thrombin (Z-Gly-Gly-Arg) was automatically added. α_2-Macroglobulin–thrombin was used separately for calibration according to the manufacturer's speci cations (Thermo Fisher Scienti c). FXa generation was performed equally but with the uorogenic substrate Pefa uor FXa (Loxo GMBH) and

resuspended in RPMI medium containing 10% FCS and stimulated with ADP or baicalein for 30 min at 37°C. Then, cells were washed and resuspended in HBSA bu er, and cell lysates were generated by three repeated freeze-thaw cycles. Samples were stored at −80°C until further analysis.

Western blotting

Cells were washed twice with PBS and then lysed in radioimmunoprecipitation assay (RIPA) bu er (50 mM Tris, 150 mM NaCl, 1 mM EDTA, 1% Triton X-100, 1% sodium deoxycholate, and 0.1% SDS) containing 1% protease/phosphatase inhibitor (P9599; Sigma-Aldrich) and 1 mM PMSF (Active Motif) for 30 min on ice. Aortas were rinsed three times with PBS containing 1,000 IU heparin, cut into little pieces, and digested in serum-free DMEM containing 2 mg/ml collagenase type 2 (Worthington Biochemical Corporation) for 1 h at 37°C and then lysed in RIPA bu er for 30 min on ice. Protein content was assessed using a BCA Protein Assay kit (Thermo Fisher Scienti c) according to the manufacturer's speci cations. Protein extracts were separated by SDS-PAGE using a 10% SDS-polyacrylamide gel, transferred to a Trans-Blot Nitrocellulose membrane (Bio-Rad Laboratories), and immunoblotted overnight in TBS-Tween containing 5% nonfat dry milk with the following antibodies: rabbit polyclonal anti–12-LO (ab23678; dilution 1:1,000; Abcam), mouse coagulation factor III/TF antibody (no. AF3178; dilution 1:200; R&D Systems), and rabbit anti–mouse β-actin (clone AC-74; dilution 1:1,000; Sigma-Aldrich). As a positive control for TF expression, lysates of LPS-treated RAW 264.7 mouse macrophages were used. As a positive control for 12/15-LO, mouse-resident macrophages were isolated from

with a ow rate of 200 µl/min. Lipids were monitored using multiple reaction–monitoring mode. Transitions monitored were for parent ions of m/z 738.6, 764.6, 766.6, and 782.6 [M−H]− fragmenting to daughter ions with m/z 219.2 (15-HETE), 115.1 (5-HETE), or 179.1 (12-HETE). Standard curves were generated using internal standards (DMPE) and di erent synthetic primary standards. Products were quanti- ed by LC/MS/MS electrospray ionization on an Applied Biosystems 4000 Q-Trap system. Acquisition of product ion spectra was triggered during elution of ions of interest, with the instrument operating in ion trap mode.

Free eicosanoid quantitation using LC/MS/MS

Lipids were separated on a C18 Spherisorb ODS2 column (150 × 4.6 mm; 5 µm particle; Waters Ltd) using a gradient of 50–90% B over 30 min, followed by 5 min at 90% B (A, water/acetonitrile/acetic acid, 75:25:0.1; B, methanol/acetonitrile/acetic acid, 60:40:0.1) with a ow rate of 1 ml/min. Eicosanoid species were monitored with speci c parent to daughter ion transitions in negative ion mode ([M−H]−) for HETEs (m/z 319.2) at 115 (5-HETE), 179.1 (12-HETE), 219 (15-HETE), 155 (8-HETE), and 167 (11-HETE). 15-HETE-d8 was monitored at m/z 327 to 226. Products were identi ed and quanti ed using primary standards, and internal standard runs in parallel under the same method conditions.

Quanti□cation of externalized aminophospholipids

Externalization of PE and PS species in eosinophils was measured according as previously described (Thomas et al., 2014). In brief, cultured mouse eosinophils (4×10^6 per ml) were stimulated with ADP (40 µM) or the calcium ionophore A23187 (10 µM) and treated with EZ-link NHS-biotin or EZ-link sulfo-NHS-biotin (Thermo Fisher Scienti c) for measuring total cellular lipids and external aminophospholipids, respectively, by LC/MS/MS.

Generation of liposomes

Liposomes used in the thrombin generation experiments contained 20% of the indicated oxidized or unoxidized phospholipid species and 75% PAPC and 5% PAPS as carrier lipids. Phospholipids were solved in methanol or chloroform and kept under a layer of argon on −80°C until usage.

Phospholipids used were: PAPS (110670; Avanti Polar Lipids, Inc.), 1-hexadecanoyl-2-(5Z,8Z,11Z,14Z-eicosatetraenoyl)-*sn*-glycero-3-phospho-l-serine PAPE (110638; Avanti Polar Lipids, Inc.), 1-hexadecanoyl-2-(5Z,8Z,11Z,14Z-eicosatetraenoyl)-*sn*-glycero-3-phosphoethanolamine PAPC (850459C; Avanti Polar Lipids, Inc.), and 1-hexadecanoyl-2-(5Z,8Z,11Z,14Z-eicosatetraenoyl)-*sn*-glycero-3-phosphocholine 12-HETE-PE. Lipids were generated as previously described (Morgan et al., 2010).

Indicated phospholipids were added to PAPC/PAPS carrier lipids before solvent was evaporated under a gentle stream of Argon. Phospholipids were resuspended in HBSA bu er and generously vortexed. Then, liposomes were prepared by 10 freeze-thaw cycles and kept on ice before performing the assay.

N. Mackman, S. Massberg, M. Rauh, K.R. Zellner, J.L. Nadler, and G. Schett helped to design the study and provided important technical input. J.J. Lee and V.B. O'Donnell helped to design the study and wrote the manuscript. G. Krönke designed the study and wrote the manuscript. All authors read and commented on the manuscript.

[redacted] 2016
: 12 F [illegible] 2017
A [illegible] : 19 A[illegible] 2017

REFERENCES

Ames, P.R., M. Margaglione, S. Mackie, and J.D. Alves. 2010. Eosinophilia and thrombophilia in churg strauss syndrome: a clinical and pathogenetic overview. *Clin. Appl. Thromb. Hemost.* 16:628–636. http://dx.doi.org/10.1177/1076029609348647

Assarsson, E., M. Lundberg, G. Holmquist, J. Björkesten, S.B. Thorsen, D. Ekman, A. Eriksson, E. Rennel Dickens, S. Ohlsson, G. Edfeldt, et al. 2014. Homogenous 96-plex PEA immunoassay exhibiting high sensitivity, speci city, and excellent scalability. *PLoS One.* 9:e95192. http://dx.doi.org/10.1371/journal.pone.00x

Nemerson, Y. 1968. The phospholipid requirement of tissue factor in blood coagulation. *J. Clin. Invest.* 47:72–80. http://dx.doi.org/10.1172/JCI105716

O'Donnell, V.B., R.C. Murphy, and S.P. Watson. 2014. Platelet lipidomics: modern day perspective on lipid discovery and characterization in platelets. *Circ. Res.* 114:1185–1203. http://dx.doi.org/10.1161/CIRCRESAHA.114.301597

Riegger, J., R.A. Byrne, M. Joner, S. Chandraratne, A.H. Gershlick, J.M. Ten Berg, T. Adriaenssens, G. Guagliumi, T.C. Godschalk, F.J. Neumann, et al. Prevention of Late Stent Thrombosis by an Interdisciplinary Global European E ort (PRESTIGE) Investigators. 2016. Histopathological evaluation of thrombus in patients presenting with stent thrombosis. A multicenter European study: a report of the prevention of late stent thrombosis by an interdisciplinary global European e ort consortium. *Eur. Heart J.* 37:1538–1549. http://dx.doi.org/10.1093/eurheartj/ehv419

Rossaint, J., D. Vestweber, and A. Zarbock. 2013. GDF-15 prevents platelet integrin activation and thrombus formation. *J. Thromb. Haemost.* 11:335–344. http://dx.doi.org/10.1111/jth.12100

Rothenberg, M.E., and S.P. Hogan. 2006. The eosinophil. *Annu. Rev. Immunol.* 24:147–174. http://dx.doi.org/10.1146/annurev.immunol.24.021605.090720

Stegemann, C., R. Pechlaner, P. Willeit, S.R. Langley, M. Mangino, U. Mayr, C. Menni, A. Moayyeri, P. Santer, G. Rungger, et al. 2014. Lipidomics pro ling and risk of cardiovascular disease in the prospective population-based Bruneck study. *Circulation.* 129:1821–1831. http://dx.doi.org/10.1161/CIRCULATIONAHA.113.002500

Stevens, G., M. Mascarenhas, and C. Mathers. 2009. Global health risks: progress and challenges. *Bull. World Health Organ.* 87:646. http://dx.doi.org/10.2471/BLT.09.070565

Suzuki, J., M. Umeda, P.J. Sims, and S. Nagata. 2010. Calcium-dependent phospholipid scrambling by TMEM16F. *Nature.* 468:834–838. http://dx.doi.org/10.1038/nature09583

Tani, Y., Y. Isobe, Y. Imoto, E. Segi-Nishida, Y. Sugimoto, H. Arai, and M. Arita. 2014. Eosinophils control the resolution of in ammation and draining lymph node hypertrophy through the proresolving mediators and CXCL13 pathway in mice. *FASEB J.* 28:4036–4043. http://dx.doi.org/10.1096/fj.14-251132

Thomas, C.P., L.T. Morgan, B.H. Maskrey, R.C. Murphy, H. Kühn, S.L. Hazen, A.H. Goodall, H.A. Hamali, P.W. Collins, and V.B. O'Donnell. 2010. Phospholipid-esteri ed eicosanoids are generated in agonist-activated human platelets and enhance tissue factor-dependent thrombin generation. *J. Biol. Chem.* 285:6891–6903. http://dx.doi.org/10.1074/jbc.M109.078428

Thomas, C.P., S.R. Clark, V.J. Hammond, M. Aldrovandi, P.W. Collins, and V.B. O'Donnell. 2014. Identi cation and quanti cation of aminophospholipid molecular species on the surface of apoptotic and activated cells. *Nat. Protoc.* 9:51–63. http://dx.doi.org/10.1038/nprot.2013.163

Tian, Y., R. Schreiber, and K. Kunzelmann. 2012. Anoctamins are a family of $Ca2^{+}$-activated Cl^{-} channels. *J. Cell Sci.* 125:4991–4998. http://dx.doi.org/10.1242/jcs.109553

Todd, S., C. Hemmaway, and Z. Nagy. 2014. Catastrophic thrombosis in idiopathic hypereosinophilic syndrome. *Br. J. Haematol.* 165:425. http://dx.doi.org/10.1111/bjh.12729

Uderhardt, S., and G. Krönke. 2012. 12/15-lipoxygenase during the